Passive diamagnetic contactless suspension rotor with electrostatic glass motor

Yuanping Xu[1], *Jin Zhou*[1] ✉, *Hannes Bleuler*[2], *Ryosuke Kan*[3]

[1]*College of Mechanical and Electrical Engineering, Nanjing University of Aeronautics and Astronautics, Nanjing 210016, People's Republic of China*
[2]*Laboratory of Robotic Systems, École Polytechnique Fédérale de Lausanne, Lausanne 1015, Switzerland*
[3]*Department of Mechanical Engineering, University of Tokyo, Tokyo 113-8656, Japan*
✉ *E-mail: zhj@nuaa.edu.cn*

Published in Micro & Nano Letters; Received on 8th March 2019; Revised on 16th April 2019; Accepted on 15th May 2019

In this work, we introduce a newly developed passive and frictionless diamagnetic contactless suspension rotor with electrostatic glass motor. A 20 mm diameter disc-shaped rotor comprised of pyrolytic graphite with glass is fabricated. The rotor is diamagnetically and passively levitated by an array of Nd–Fe–B magnets at room temperature without any energy supply. To realise the rotating function, a 700 V high voltage electrostatic glass motor is designed and arranged in the levitation air gap between the rotor and the magnets. To install the stator in this narrow air gap, we fabricated the stator using a flexible printed circuit with 100 μm thickness. The newly developed system is more compact, stable and of high performance. The maximum speed has been improved doubly to 300 rpm in atmosphere. We intend to draw attention to this uncommon levitation and to show that it could be used for micro-mechatronic system.

1. Introduction: Magnetic bearing technologies have been increasingly applied in compressors, pumps, and many other high-speed rotating types of machinery owing to the contactless, non-lubrication and high-efficiency merits. For the conventional magnetic bearing system, the frictionless levitation is often achieved by means of feedback controlled electromagnetics [active magnetic bearing, (AMB)], but the disadvantage for AMB is that the realisation micro size is challenging. Since the air gap between stator and rotor is relatively large compared to the rotor with scale downsizing and coils have to be placed relatively far from the rotor, leakage flux will become huge for micro active magnetic bearings [1]. Therefore, other levitation forms such as electrostatic levitation, acoustic levitation, and passive magnet levitation are employed for micro system.

Passive magnetic levitation could overcome the scale downsizing and complexity difficulty. Compared with other passive magnetic levitation principles, the diamagnetic levitation is the only one which could realise completely passive and static stable levitation at room temperature since diamagnetic materials are repelled by a magnetic field [2, 3]. More importantly, diamagnetic levitation can stably operate without external energy input with significant advantages for the energetic efficiency improvement [4]. The shortcoming of the diamagnetic levitation is the weakness of the diamagnetic effect which hinders the development and application of this technology. However, in recent years, with the development of strong magnetic field equipment and micro technology, increasing publications on diamagnetic levitation research focusing on different fields are appearing.

Normally there are two distinct systems using diamagnetic levitation forms: (i) the magnets are levitated by diamagnetic materials; (ii) the diamagnetic material is levitated by magnets or magnetic field. Both of them are potentially useful and many works have been reported. Berry and Geim diamagnetically levitated a live frog under a 16 T strong magnetic field using the weak repulsive forces operating between magnets and diamagnetic properties of living tissue [5, 6]. Su *et al.* calculated and verified the nonlinearity characteristics of a diamagnetic levitation structure [7]. Rikken *et al.* reported the exploration of diamagnetic repulsion forces for the selective manipulation of micro particles inside microfluidic devices [8]. Billot *et al.* presented an estimation and a passive compensation strategy for nanoforce sensor based on diamagnetic levitation [9]. Gao *et al.* presented a bistable vibration energy harvester using diamagnetic levitation principle [10]. Palagummi and Yuan reported a horizontal diamagnetic levitation mechanism for low-frequency vibration energy harvesting [11]. Pelrine *et al.* firstly suggested diamagnetically levitated micro robots and reported the levitation of micro-robots with unusual motion properties [12, 13]. Hsu *et al.* proposed the application of micro-robots for building carbon fibre trusses using diamagnetic micro-manipulation [14].

In the rotating types of machinery field, Cansiz diamagnetically levitated a disk-shaped Nd–Fe–B permanent magnet rotor with the arrangement of ferrite magnet and bismuth blocks and the rotor was accelerated by a cold gaseous nitrogen jet [15]. Su *et al.* diamagnetically levitated a highly oriented pyrolytic graphite rotor and accelerated by gas to a maximum rate of 500 rpm [16]. The above references focus on the diamagnetic bearing properties and the rotor is powered by the gas. For the 'active' rotation realisation, Moser and Bleuler proposed a concept to combine the diamagnetic levitation and electrostatic glass motor together to fulfil the rotation function [17]. Liu *et al.* levitated a gear-shaped pyrolytic graphite rotor and adopted a three-phase axial variable-capacitance motor to drive the rotor. Also a maximum speed over 10 rpm in the atmosphere was observed [18].

Increasing the maximum speed will improve the system power density and performance. However, at present, for the diamagnetic rotor system with micro shape and light mass, the active rotation maximum speed reported is still low. Our previous work [19] firstly realises a rotating diamagnetically levitating rotor system driven by electrostatic field and promoted the maximum speed to 140 rpm, which have also been times faster than [18]. However, the driven stator of electrostatic glass motor is arranged on the top of the rotor disc, which introduces potential instability when the air gap between rotor and stator is too small or driven voltage is too high.

In this Letter, we report our latest developments on diamagnetic levitation bearing rotor, which solves the previous problem. The newly developed demo is more compact, stable and high performance and a maximum speed of 300 rpm has been observed in the atmosphere.

2. Principles: For the diamagnetic material with magnetisation M_d, the elementary diamagnetic force on the unit volume under the magnetic flux density B is calculated as

$$f = M_d \cdot \nabla(B) \tag{1}$$

© The Institution of Engineering and Technology 2019

doi: 10.1049/mnl.2019.0144

The magnetic flux density B and the magnetic field H are linked by following relation:

$$H = \frac{B}{\mu_0} - M_{\mathrm{d}}, \tag{2}$$

where μ_0 is the magnetic permeability of vacuum. The induced magnetisation M_{d} is related to the magnetic flux density B by the equation

$$M_{\mathrm{d}} = \chi_{\mathrm{m}} H, \tag{3}$$

where χ_{m} is the magnetic susceptibility. For the diamagnetic materials, as the χ_{m} is very small, given (2) and (3), we can express M_{d} as a function of B

$$M_{\mathrm{d}} = \frac{\chi_{\mathrm{m}}}{(1+\chi_{\mathrm{m}})\mu_0} B \simeq \frac{\chi_{\mathrm{m}}}{\mu_0} B. \tag{4}$$

Therefore, the expression of the diamagnetic force per unit volume in the function of the magnetic flux density becomes

$$f = \frac{\chi_{\mathrm{m}}}{\mu_0} B \cdot \nabla(B). \tag{5}$$

The total magnetic force acting on the diamagnetic body can be obtained by integrating the unit force on the entire volume

$$F = \frac{\chi_{\mathrm{m}}}{2\mu_0} \int_V \nabla(B^2)\, \mathrm{d}V. \tag{6}$$

For a diamagnetic material with negative magnetic susceptibility χ_{m}, when it is immersed to an external magnetic field, due to the main contribution of orbital magnetisation, the diamagnetic material creates an opposite magnetic field and the reaction force from (6) will push the diamagnetic body out of the field. Therefore, diamagnetic materials such as bismuth or graphite could be stably levitated when the potential surfaces of the magnetic field are concave (cup-like). Table 1 lists the magnetic susceptibility of some diamagnetic materials.

The electrostatic glass motor operation principle is shown in Fig. 1. For a dielectric material such as glass with low conductivity, when it is immerged to an electric field, due to the ion migration, induction charges are generated on the dielectric material surface. However, because of the low conductivity, the charges on the glass surface lag behind the stator excitation, which results in a tangential electric field that drives the glass to rotate [20].

Table 1 Magnetic susceptibility of some diamagnetic materials

Material	χ_{m} (10^{-6})
water	−9.0
bismuth	−160
pyrolytic graphite ⊥	−450
pyrolytic graphite ∥	−85
superconductor	-10^6

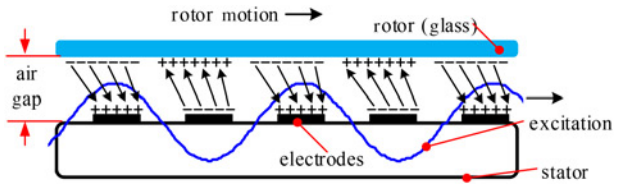

Fig. 1 *Principle of the electrostatic glass motor*

3. Device fabrication: Fig. 2 shows this novel diamagnetic rotor bearing. The planar rotor disc is stably levitated by an array of Nd–Fe–B magnets with a 500 µm air gap and powered by electrostatic glass motor.

The disc-shaped (Ø 20 mm) diamagnetic rotor is comprised of pyrolytic graphite and D263-T type borosilicate glass, which are glued concentrically. The diamagnetic levitation is provided by pyrolytic graphite disc and the glass is responsive for rotation. The thickness for the pyrolytic graphite and borosilicate glass is 500 and 120 µm, respectively. Fig. 3*a* shows the diamagnetic rotor employed in this Letter and Fig. 3*b* indicates its structure. Table 2 lists the property of D263-T type glass.

For the array of permanent magnets, a concentric ring-shaped magnet (Ø30 × Ø16 × 7 mm) encircling a cylinder magnet (Ø16 × 7 mm) with opposite axial magnetisation pattern is adopted in this Letter, which is shown in Fig. 4*a*.

The magnetic field provided by the array of permanent magnets can be evaluated by the sum of two magnets. Here, the method provided in [21] is employed to calculate the magnetic flux density. For the axially polarised ring-shaped magnet, the volume current density $\boldsymbol{J}_{\mathrm{m}} = \nabla \times M$ is zero due to the polarised magnetisation M and the surface current density is $\boldsymbol{j}_{\mathrm{m}} = M \times \hat{\boldsymbol{n}}$. Therefore, the vector potential $\boldsymbol{A}$ can be written as

$$\boldsymbol{A}(x) = \frac{\mu_0}{4\pi} \oint_{\mathrm{s}} \frac{\boldsymbol{j}_{\mathrm{m}}(x')}{|x - x'|} ds'. \tag{7}$$

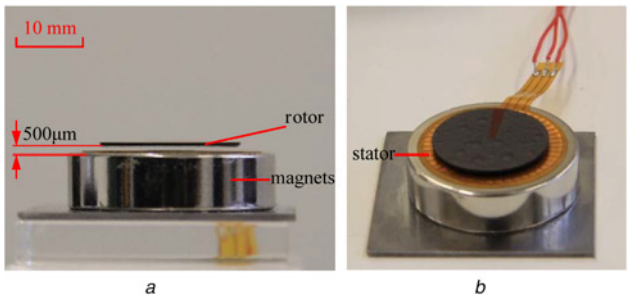

Fig. 2 *Diamagnetic rotor bearing with electrostatic glass motor*
a Side view
b Perspective view

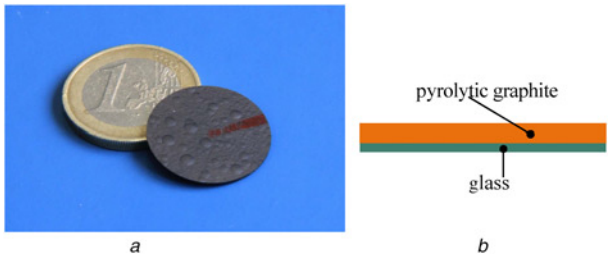

Fig. 3 *Diamagnetic rotor, comprised of pyrolytic graphite and D263-T type borosilicate glass*
a Diamagnetic rotor
b Structure

Table 2 Property of D 263-T

Name	Values
density	2.51 g/cm^3
Young's modulus	72.9 kN/mm^2
Poisson's ratio	0.208
dielectric constant	6.7 (1 MHz)

© The Institution of Engineering and Technology 2019

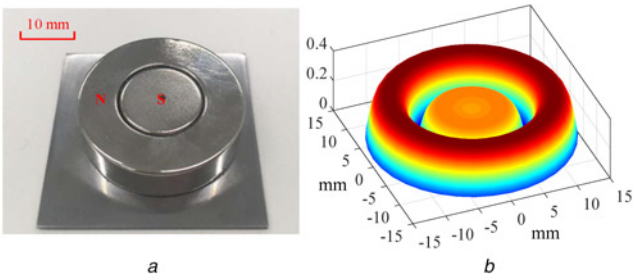

Fig. 4 *Array of magnets and the magnetic potential*
a Array of Nd–Fe–B
b Magnetic potential (B^2) for magnets arrangement

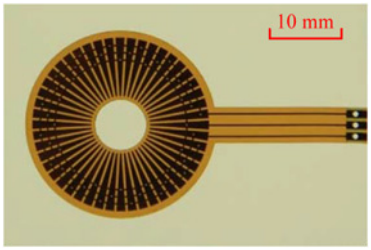

Fig. 5 *Electrostatic motor stator structure*

Since the $\boldsymbol{A}(x)$ has no z-component, it can be written in terms of cylindrical coordinates by computing the projections

$$A_r(x) = \boldsymbol{A}(x) \cdot \hat{\boldsymbol{r}}, \tag{8}$$

$$A_\phi(x) = \boldsymbol{A}(x) \cdot \hat{\boldsymbol{\phi}}. \tag{9}$$

The magnetic flux density B and vector potential $\boldsymbol{A}$ are linked by following relation

$$\boldsymbol{B} = \nabla \times \boldsymbol{A}. \tag{10}$$

Therefore, the axial field component is obtained

$$B_z(x) = \frac{1}{r}\left(\frac{\partial}{\partial r}\left(rA_\phi(x)\right) - \frac{\partial}{\partial \phi}A_r(x)\right). \tag{11}$$

Similarly, we can get the axial field component for the encircled cylinder magnet $B_{zc}(x)$. So, the total axial field component is calculated as

$$B_{zt}(x) = B_z(x) + B_{zc}(x). \tag{12}$$

The magnetic potential surface of the magnetic field array in the axial direction is evaluated with the M parameters 14×10^5 A/m for the ring magnet and 11×10^5 A/m for the encircled cylinder magnet. Fig. 4*b* shows the axial 3D view of magnetic potential (B^2) at 600 µm above the magnets calculated from the above derivation. It can be seen that the axial magnetic potential surfaces of the magnetic field are concave (cup-like), which lead to the stably diamagnetic levitation.

The electrostatic glass motor system includes signal generator, high voltage amplifiers and electrostatic stator. Since the air gap between the rotor and the magnets is limited in 500 µm (Fig. 2), it is practically impossible to use industry standard printed circuit board (PCB) (1.0–1.6 mm thickness) to be located in it. Therefore, we fabricated the stator using a flexible PCB with 100 µm thickness, which is shown in Fig. 5. The stator possesses 16 poles (48 electrodes) and a 280 µm gap between two electrodes.

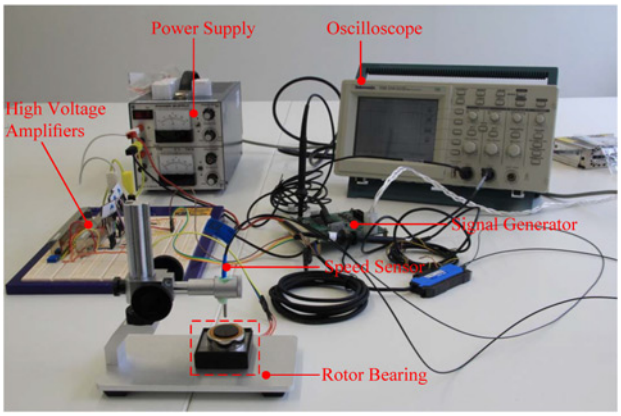

Fig. 6 *Experimental system*

4. Experiment and discussion: Fig. 6 presents the whole test rig, which include power supply, high voltage amplifier, signal generator, speed sensor, rotor bearing, and oscilloscope. The power supply proved 12 V voltage to high voltage amplifiers module and signal generator provide excitation signal to high voltage amplifiers module. For the high voltage amplifier module, THV 12-500P and THV 12-500N high voltage power supplies components from Tracopower, and PA97 high voltage amplifier components from Apex are adopted. The maximum output voltage is set from −350 to 350 V. For the signal generator module, the DSP28335 microcontroller is adopted and the sampling frequency is set 100 kHz.

The step three-phase excitation strategy is employed in the experiment. Before the run-up, a certain amount of net charges on the glass surface was built up under a static field around 10 s charging time using constant voltages (−350 V, 0 V, +350 V). After this charging period, the voltages of the three electrodes are changed and accelerated periodically in a step strategy. The speed is increased by 0.75 r/min/s from 0 to 200 rpm and by 0.25 r/min/s from 200 to 300 rpm. Maximum rotation speeds of 300 rpm have been observed and the rotor will fall out of step when losses is too high.

The diamagnetic levitation and electrostatic driven system possess energetic efficiency and micro structure merits, which have potential promising application for the micro-mechatronic system. In this work, the system maximum speed is also limited by the torque and air resistance, which may be improved continuously by the driven system parameters optimisation. Furthermore, the rotor and magnets size can be minimised to make it more compact and small. Our future studies are directed to improve the performance by optimising the parameters to make it operate in higher speed.

5. Acknowledgments: The authors thank the staff at LSRO at EPFL for technical support and the support of the China Postdoctoral Science Foundation (grant no. 2018M642245), and in part by the Jiangsu Province Key R & D Programs (grant no. BE2016180).

6 References

[1] Maslen E.H., Schweitzer G. (Eds.): 'Magnetic bearings' (Springer Berlin Heidelberg, Germany, 2009)
[2] Simon M.D., Heflinger L.O., Geim A.K.: 'Diamagnetically stabilized magnet levitation', *Am. J. Phys.*, 2001, **69**, (6), pp. 702–713
[3] Zhang K., Su Y., Ding J., *ET AL.*: 'Design and analysis of a gas flow-meter using diamagnetic levitation', *IEEE Sens. J.*, 2018, **18**, (17), pp. 6978–6985
[4] De Pasquale G., Iamoni S., Somà A.: '3D numerical modeling and experimental validation of diamagnetic levitating suspension in the static field', *Int. J. Mech. Sci.*, 2013, **68**, pp. 56–66

© The Institution of Engineering and Technology 2019

doi: 10.1049/mnl.2019.0144

[5] Berry M.V, Geim A.K.: 'Of flying frogs and levitrons', *Eur. J. Phys.*, 1997, **18**, (4), pp. 307–313
[6] Simon M.D., Geim A.K.: 'Diamagnetic levitation: flying frogs and floating magnets (invited)', *J. Appl. Phys.*, 2000, **87**, (9), pp. 6200–6204
[7] Su Y., Zhang K., Ye Z.: 'Levitation and nonlinearity characteristics of a diamagnetic levitation structure', *Int. J. Appl. Electromagn. Mech.*, 2017, **55**, (1), pp. 113–128
[8] Rikken R.S.M., Nolte R.J.M., Maan J.C., *ET AL.*: 'Manipulation of micro- and nanostructure motion with magnetic fields', *Soft Mat.*, 2014, **10**, (9), pp. 1295–1308
[9] Billot M., Piat E., Abadie J., *ET AL.*: 'External mechanical disturbances compensation with a passive differential measurement principle in nanoforce sensing using diamagnetic levitation', *Sens. Actuators A, Phys.*, 2016, **238**, pp. 266–275
[10] Gao Q.-H., Zhang W.-M., Zou H.-X., *ET AL.*: 'Design and analysis of a bistable vibration energy harvester using diamagnetic levitation mechanism', *IEEE Trans. Magn.*, 2017, **53**, (10), pp. 1–9
[11] Palagummi S.V., Yuan F.-G.: 'An enhanced performance of a horizontal diamagnetic levitation mechanism–based vibration energy harvester for low frequency applications', *J. Intell. Mater. Syst. Struct.*, 2017, **28**, (5), pp. 578–594
[12] Pelrine R.E.: 'Room temperature, open-loop levitation of micro-devices using diamagnetic materials'. IEEE Proc. on Micro Electro Mechanical Systems, CA, USA, February 1990, pp. 34–37
[13] Pelrine R., Wong-Foy A., McCoy B., *ET AL.*: 'Diamagnetically levitated robots: an approach to massively parallel robotic systems with unusual motion properties'. IEEE Int. Conf. on Robotics and Automation, Saint Paul, USA, May 2012, pp. 739–744
[14] Hsu A., Wong-Foy A., McCoy B., *ET AL.*: 'Application of micro-robots for building carbon fiber trusses'. Int. Conf. on Manipulation, Automation and Robotics at Small Scales, Paris, France, July 2016, pp. 1–6
[15] Cansiz A.: 'Static and dynamic analysis of a diamagnetic bearing system', *J. Appl. Phys.*, 2008, **103**, (3), p. 034510
[16] Su Y., Xiao Z., Ye Z., *ET AL.*: 'Micromachined graphite rotor based on diamagnetic levitation', *IEEE Electron Device Lett.*, 2015, **36**, (4), pp. 393–395
[17] Moser R., Bleuler H.: 'Precise positioning using electrostatic glass motor with diamagnetically suspended rotor', *IEEE Trans. Appil. Supercond.*, 2002, **12**, (1), pp. 937–939
[18] Liu W., Chen W.-Y., Zhang W.-P., *ET AL.*: 'Variable-capacitance micromotor with levitated diamagnetic rotor', *Electron. Lett.*, 2008, **44**, (11), p. 681
[19] Xu Y., Cui Q., Kan R., *ET AL.*: 'Realization of a diamagnetically levitating rotor driven by electrostatic field', *IEEE/ASME Trans. Mechatronics*, 2017, **22**, (5), pp. 2387–2391
[20] Livermore C., Forte A.R., Lyszczarz T., *ET AL.*: 'A high-power MEMS electric induction motor', *J. Microelectromech. Syst.*, 2004, **13**, (3), pp. 465–471
[21] Furlani E.P.: 'Permanent magnet and electromechanical devices' (Elsevier, USA, 2001)

© The Institution of Engineering and Technology 2019